New Phytologist

Research

Physiological responses of *Catharanthus roseus* (periwinkle) to ash yellows phytoplasmal infection

Puay Yok Tan and Thomas Whitlow

Department of Horticulture, Cornell University, Ithaca, New York 14853, USA

Author for correspondence:
Thomas Whitlow
Tel.: +1 607 255 1787
Fax: +1 607 255 9998
Email: thw2@cornell.edu

Received: *15 September 2000*
Accepted: *10 January 2001*

Summary

• Photosynthetic responses of periwinkle (*Catharanthus roseus*) were compared during disease development after infection by two strains of ash yellows (AshY) phytoplasmas that differed in aggressiveness.

• Healthy plants were inoculated by grafting with diseased scions. Mature leaves formed before grafting of diseased scion, and leaves formed during disease development were monitored for physiological changes.

• Leaves formed before inoculation remained visually and physiologically asymptomatic until normal senescence. However, leaves formed after inoculation had reduced photosynthesis, due to reductions in both the maximum carboxylation rate (Vc_{max}) and noncyclic electron transport (J_{max}). In these leaves, photoinhibition resulted from photoprotective processes rather than photooxidative damage to PSII reaction centres. Stomatal conductance (G_s) was reduced, but this did not increase the stomatal limitation to photosynthesis. Changes in G_s were not correlated with changes in leaf ABA concentration.

• Known differences in phytoplasmal aggressiveness were correlated with degrees of inhibition of photosynthesis and occurence of photoinhibition. AshY phytoplasmas appear to cause metabolic perturbations associated with localized accumulation or multiplication of the pathogen in symptomatic leaves.

Key words: *Catharanthus roseus* (periwinkle), phytoplasma, ash yellows, leaf gas exchange, biochemical limitation, stomatal limitation, chlorophyll fluorescence, chlorophyll content.

Abbreviations

A, net photosynthesis rate; A_a, net photosynthesis rate at ambient [CO_2]; A_{max}, net photosynthesis rate at saturated [CO_2]; AshY, ash yellows; C_i, intercellular [CO_2]; F_o, F_m, F_v, minimal, maximum and variable fluorescence, respectively; F'_m, F_s, maximal and steady state fluorescence in light-adapted state; F_v/F_m, intrinsic efficiency of PSII; G_s, stomatal conductance; J_{max}, maximum noncyclic electron transport; L_s, stomatal limitation; Φ_{PSII}, quantum yield of PSII; q_{NP}, nonphotochemical quenching coefficient; RuBP, ribulose-1,5-biophosphate; Vc_{max}, maximum rate of carboxylation of Rubisco; vpd, leaf-to-air vapor pressure deficit; WAG, week after grafting.

Introduction

Ash yellows (AshY) is a disease of *Fraxinus* spp. and *Syringa* spp. (Sinclair & Griffiths, 1994; Sinclair *et al.*, 1996) caused by phytoplasmas belonging to a group for which the name of '*Candidatus* Phytoplasma fraxini' has been proposed (Griffiths *et al.*, 1999). Growth studies on periwinkle, and green ash, *Fraxinus pennslyvanica*, infected with different strains of AshY phytoplasmas collected from naturally infected plants in 16 localities (Sinclair *et al.*, 1997) indicate a continuum of

aggressiveness among different strains (Sinclair & Griffiths, 2000). Likewise, phytoplasmas in different taxa exhibited varying aggressiveness when the same plant genotype was infected (Lepka *et al.*, 1999). The underlying causes of differences in aggressiveness between strains within and between groups remain largely unknown, as do the bases of pathogenicity (Sinclair & Griffiths, 2000). The current inability to culture phytoplasmas under axenic conditions has led to limited knowledge of their physiological and biochemical properties. However, the study of events downstream of the initial infection processes can provide useful insight into characteristics of their pathogenesis.

In this study, we monitored the physiological changes in leaves formed before and after inoculation by grafting, with a focus on photosynthetic characteristics under the influence of a less virulent (AshY2) and a more virulent (AshY5) strain belonging to the same phytoplasmal taxon. AshY infection of *Fraxinus* leads to impaired photosynthesis (Sinclair & Griffiths, 1997), as is the case in other phytoplasmal diseases (León *et al.*, 1996; Samaddar *et al.*, 1996). However, it is not certain if impaired photosynthesis results from stomatal or biochemical limitation, or a combination of both. In this study, the use of 'stomatal limitation' is as described in Farquhar & Sharkey (1982). Stomatal limitation occurs even in nonstressful growth conditions in the sense that actual photosynthetic rates are lower than the maximum rates possible when stomatal and other resistances to CO_2 diffusion are negligible. Concurrent reductions in stomatal conductance and photosynthesis do not necessarily lead to an increased stomatal limitation, unless there is a corresponding decrease in intercellular (substomatal) CO_2 concentration (C_i) (Farquhar & Sharkey, 1982). Reduced stomatal conductance, which has been reported to be an early and consistent symptom following infection (Matteoni & Sinclair, 1983; León *et al.*, 1996), may or may not impose an increased stomatal limitation on photosynthesis. Biochemical limitations of photosynthesis could arise from a reduction in carboxylation capacity, regeneration of RuBP (von Caemmerer & Farquhar, 1981), or triose phosphate utilization rate for regeneration of inorganic phosphate (Pi) (Sharkey, 1989; Sage, 1994).

There is currently no information on the relative contributions of stomatal and biochemical limitations of photosynthesis in phytoplasmal diseases. The first objective of the study was to test the hypothesis that stomatal limitation arising from reduced stomatal conductance is responsible for the decline in photosynthesis early in disease development, and biochemical limitations become relatively more important in the later stages. With increased limitation of the dark reactions of photosynthesis during disease development, it is expected that photon absorption eventually exceeds the capacity of the dark reactions to utilize the products of light-driven electron transport, leading to a reduction in the quantum yield of photochemistry, termed photoinhibition (Krause, 1988). Photoinhibition has both a photoprotective component, involving a reversible alteration in the reaction centres of PSII and dissipation of excess photon as heat, and a photoinhibitory component involving damage to the D1 protein of PSII reaction centres and transformation of the PSII reaction centres to nonfunctional energy traps. Infection with tobacco mosaic virus predisposes tobacco leaves to photoinhibitory damage (Balachandran & Osmond, 1994), whereas in peach leaves infected with *Taphrina deformans*, photoprotective mechanisms were responsible for the decline in quantum yield of photochemistry (Raggi, 1995). There is no information on the nature of photoinhibition that may occur in phytoplasmal diseases. The second objective was to determine if photoinhibition occurs and to characterize the nature of photoinhibition during pathogenesis using Chl fluorescence quenching analysis, which is widely used to examine the energy fluxes in the photosynthetic apparatus and photoinhibition (Krause & Weis, 1991).

Phytoplasmas in plants are thought to be limited to the phloem sieve elements (Davis & Lee, 1982). As with many plant viruses (Leisner & Turgeon, 1993; Gilbertson & Lucas, 1996), a systemic infection involves the movement of phytoplasmas in the network of phloem sieve tubes, in directions determined by the relative strengths of the major sinks. Therefore, it is predicted that relatively few phytoplasma cells will enter leaves that are already mature at the time of infection. However, it is uncertain if physiological functions of mature leaves are affected in the absence of localized accumulation of phytoplasmas. These functions could be affected by a xylem-translocated pathogen-induced or pathogen-derived metabolite or toxin. Studies involving rice yellow dwarf (Nakashima & Hayashi, 1995), Australian papaya dieback (Siddique *et al.*, 1998) and lethal yellowing of palms (León *et al.*, 1996) indicate the involvement of translocated metabolites that cause symptoms in mature leaves and in tissues where the phytoplasma titre is low. In aster yellows (Kuske & Kirkpatrick, 1992) and X disease (Douglas, 1986), the severity of symptom expression is correlated with the titre of phytoplasma in the tissue, which indicates a localized effect of phytoplasma. The third objective of our study was to ascertain if AshY phytoplasmas act through a local effect or at a distance from responding tissues.

Materials and Methods

Plant materials and treatments

Periwinkle (*Catharanthus roseus* (L.) G. Don cv. Little Pinkie) were grown from cuttings and transplanted to 3.8 l pots containing mixture of equal volumes of soil and peat moss. Inoculation was carried out by grafting healthy plants with 8-cm long symptomatic scions taken from two stock plants infected with two AshY strains: AshY2 (low aggressiveness) and AshY5 (higher aggressiveness) (Sinclair & Griffiths, 2000). Control plants were grafted with scions from healthy plants. Two top-wedge grafts were done per plant for a total of five plants per treatment. Grafting was repeated on two of five

healthy plants due to graft failure. The glasshouse was maintained at 25°C daytime and 18°C nighttime, 50–60% rh, and a 14-h photoperiod. Plants were watered daily and fertilized every 2 wk with EXCEL (Scott-Siera Horticultural Products, Marysville, OH, USA) 15–15–15 at 300 μmol mol^{-1} of each nutrient. Physiological measurements began 1 wk after grafting (WAG). To detect phytoplasmas, root sections were taken from the diseased treatments 6 and 15 WAG and examined using the DAPI (4′,6-diamidino-2-phenylindole·2HCl) fluorescence test (Seemüller, 1976).

Gas exchange

For each experimental plant, a mature leaf two nodes below the graft union (fifth or sixth node from the shoot tip) was selected for measurement using an open-flow gas exchange system (Li-Cor 6400, Li-Cor Inc, Lincoln, NE, USA) fitted with the standard leaf chamber and CO_2 injector system (model 6400–01, Li-Cor). Measurements were made on well-watered plants under a light a level of 1000–1100 μmol m^{-2} s^{-1}, which was initially determined from a light response curve as sufficient to saturate photosynthesis at ambient [CO_2] (360 μmol mol^{-1}). The light was provided from a tungsten halogen lamp, which passed through a 5-cm thick chilled circulating water bath in a clear polycarbonate container. During measurements, the leaf temperature was kept at 25 ± 0.5°C and vapor pressure deficit (vpd) kept at 1.2 ± 0.1 kPa. Net photosynthesis rate (A) vs intercellular (substomatal) [CO_2] (C_i) response curves (A/C_i curves) were obtained by varying the [CO_2] in the leaf chamber stepwise in this order: 360, 250, 150, 50, 360, 450, 550, 650, 750, 900, 1100, 1300, 1700 μmol mol^{-1}, with 4–5 min given for equilibration at each [CO_2]. Analysis of the stomatal limitation index (L_s) was calculated from the A/C_i curves based on Farquhar & Sharkey (1982), in which:

$$L_s = 100\ (A_o - A_a)/A_o \qquad \text{Eqn 1}$$

(A_a, net photosynthesis rate measured at ambient [CO_2]; and A_o, the net photosynthesis rate that would occur if stomata were fully open, that is where C_i equals ambient [CO_2].) A quadratic function was fitted to each A/C_i curve with C_i in the range of 0–750 μmol mol^{-1}. In all curves fitted, the quadratic functions explained 98–99% percent of the variation in the A/C_i data. The quadratic functions were used to estimate A_o and A_{max}. A_a was obtained by averaging the two net photosynthesis rates obtained from the gas exchange measurements.

Estimates of the maximum rate of carboxylation (Vc_{max}), that is carboxylation under the conditions of saturated CO_2 and ribulose-1,5-bisphosphate (RuBP) and fully activated Rubisco, and the maximum electron transport capacity (J_{max}) were obtained by fitting the biochemical model of von Caemmerer & Farquhar (1981) to the A/C_i curves. The model allows a mechanistic interpretation of the gas exchange data and assessment of the above biochemical components of photosynthesis under the effects of the disease. In the model, A is related to C_i by the equation:

$$A = -R_{day} + \min\{W_c, W_j\}(1 - \Gamma^*/C_i) \qquad \text{Eqn 2}$$

(R_{day}, day respiration (release of CO_2 in the light by processes other than photorespiration); and Γ^* is the CO_2 compensation point in the absence of R_{day}.) Without considering inorganic phosphate limitation on the regeneration of RuBP, the rate of carboxylation is limited by the lesser of two variables, W_c and W_j. W_c represents the limitation on the rate of carboxylation imposed by the capacity of Rubisco to carboxylate RuBP. W_j represents the limitation on the rate of carboxylation imposed by the capacity for noncyclic electron transport in the thylakoids for the production ATP and NADPH, which are needed for the regeneration of RuBP. W_c and W_j are related to Vc_{max} and J_{max} by functions:

$$W_c = (Vc_{max} \cdot C_i)/[(C_i + K_c(1 + O/K_o)] \qquad \text{Eqn 3}$$

and

$$W_j = J \cdot C_i/[4(C_i + 2\Gamma^*)] \qquad \text{Eqn 4}$$

(K_c, the Michaelis–Menten constant for carboxylation; K_o, the Michaelis–Menten constant for oxygenation; and O, the partial pressure of O_2.) J is the rate of electron transport, and is related to a given irradiance, I by:

$$J = (J_{max} \cdot I)/(I + 2.1J_{max}) \qquad \text{Eqn 5}$$

Following Geber & Dawson (1997), the following parameter values were used for the nonlinear regression curve fitting using PROC NLIN (SAS Institute, Cary, NC, USA): K_c, 310 μmol CO_2 mol^{-1} air and K_o, 210 mmol O_2 mol^{-1} air. Vc_{max} and J_{max} were estimated simultaneously from the entire range of A/C_i values using the Marquardt method of iteration. The fitted biochemical model explained 95–99% of the variation for all the A/C_i data. We did not include the inorganic phosphate limitation factor in the model, as the inclusion of this factor will only marginally increase the proportion of variation in the data explained by the model, given the relatively high R^2 values that we have obtained (see Harley *et al.*, 1992).

Chl fluorescence measurements

Chl fluorescence measurements were made on the middle upper surface of a mature leaf using a pulse-modulated fluorometer (FMS2, Hansatech, King's Lynn, UK) at ambient [CO_2] and ambient temperature. Fluorescence levels with all the PSII reaction centres open and electron acceptors fully oxidized (minimal fluorescence, F_o), and reaction centres closed and electron acceptors fully reduced (maximal fluorescence, F_m)

were measured on leaves dark-adapted for 10 min using FMS2 leaf clips. Maximal fluorescence was induced by a saturating pulse of light (approx. 15 000 μmol m^{-2} s^{-1}) applied over 0.7 s. F_o was measured as the average of the fluorescence signal under a weak pulse of amber modulating light emitting diode (LED) light over a 1.8 s period, and F_m was obtained after a saturating pulse of 0.7 s. The maximum quantum efficiency of PSII was determined as F_v/F_m, where F_v (variable fluorescence) is the difference between F_o and F_m. An actinic light source (1980 μmol m^{-2} s^{-1}) was then applied for 400 s to achieve steady state photosynthesis and to obtain F_s (steady state fluorescence yield), after which a second saturation pulse was applied for 0.7 s to obtain F'_m (light adapted maximum fluorescence). The quantum efficiency of PSII (Φ_{PSII}) was determined as $\Phi_{PSII} = (F'_m - F_s)/F'_m$ (Genty *et al.*, 1989). Other fluorescent parameters were calculated by FMS2 based on the dark adapted and light adapted fluorescence measurements: q_P (photochemical quenching coefficient) $= (F'_m - F_s)/(F'_m - F_o)$; q_{NP} (non-photochemical quenching coefficient) $= (F_m - F'_m)/(F_m - F_o)$ (Schreiber *et al.*, 1986).

Leaf Chl and N content measurements

Nondestructive measurement of leaf Chl content was first obtained indirectly using a Minolta Chl meter (model SPAD-502, Minolta, Japan) by averaging of three readings along the length of a leaf. The SPAD readings were converted to Chl content (mg cm^{-2}) using a SPAD-Chl content calibration curve. Chl extraction was performed using *N,N*-dimethylformamide (DMF), with a leaf fr. wt: extraction solution ratio of about 1 : 12.5 (w/v) (Moran & Porath, 1980). Leaf discs were extracted in DMF in the dark at 4°C for 48 h and Chl content in the extract determined spectrophometrically using the equation of Moran (1982). The final calibration curve for conversion of SPAD readings to Chl content explained 92% of the total variation of the SPAD readings. Total N for leaf tissue was determined from about 5 mg d. wt by combustion analysis (Dumas method), using a NC 2100 Combustion Analyzer (CE Instruments, CE Elantech, NJ, USA). Total leaf N was expressed as percentage of d. wt.

ABA assay

Leaf ABA content was determined using an indirect enzyme-linked immunosorbent assay (ELISA) method modified from Ober *et al.* (1991). Leaf discs were collected from fully expanded leaves between 15.00 and 16.00 h from well-watered plants. ABA was extracted from leaf tissue samples (1 : 12.5 f. wt/v) with 80% (v/v) aqueous methanol containing 10 mg l^{-1} butylated hydroxytoluene and 1% (v/v) glacial acetic acid. The samples were stored at –20°C until the time of assay. The extracts were purified using reverse-phase C18 columns containing about 0.15 g of 40 μm particle size packing material (bonded-phase octadecylsilane, J. T. Baker Chemicals, Phillipsburg, NJ, USA). A test of the amount of ABA recovered using the purification method using [^{3}H]-ABA indicated that about 95% of the ABA was recovered. The indirect ELISA method used commercial monoclonal antibodies specific for (S)-ABA (Idetek, San Bruno, CA, USA), and secondary antibody and ABA standards from Sigma Chemical Co, MO, USA.

Sampling methods

A/C_i, SPAD, and Chl fluorescence measurements were obtained initially from the same mature leaf two nodes below the graft union in each experimental plant from 1 to 9 WAG. Around 9 WAG, the monitored leaves began to senesce. Therefore, from 11 WAG onwards, symptomatic leaves on the fifth or sixth node from the shoot tip formed during pathogenesis were monitored until 19 WAG. Leaves for ABA and leaf nitrogen analysis were selected from the corresponding (pre- or postgrafting) leaves at the fifth or sixth node below the shoot tip at each monitoring period.

Statistical analyzes

Treatments and plants in the experiment were completely randomized. One-way ANOVA was performed using general linear model procedure (PROC GLM) of SAS (SAS Institute, Cary, NC, USA) to determine the significance of treatment effect each week of measurement. Tukey honestly significant difference (HSD) multiple comparison procedure was used to compare treatment means within weeks when significant treatment effects were detected. Values shown in figures and tables are means of three replicates. For the analysis of the stomatal conductance vs. leaf-to-air vapor pressure deficit relation, linear regression analysis using PROC GLM (SAS Institute) was used to assess the significance of the linear functions, and of differences between the regression slope values. The ANOVA assumptions of homogeneity of variance and normality of residuals of the linear model were checked for all data analyzes.

Results

Establishment of systemic infection

Graft unions were successfully established after about 2 wk. Phytoplasmas were detected in small quantities in root sections of the phytoplasma-inoculated plants on 6 WAG using DAPI. In two of the AshY2 treatment plants and one of AshY5 treatment plants, phytoplasma were not detected, and these plants failed to develop symptoms. Chlorosis, the first visual symptom of pathogenesis, developed in leaves formed after grafting about 8 WAG in the AshY2 treatment, and 9 WAG in the AshY5 treatment. Plants from which phytoplasmas were not detected were not used for the analysis. By 11 WAG, shoots with witches' brooms appearance arizing from proliferation

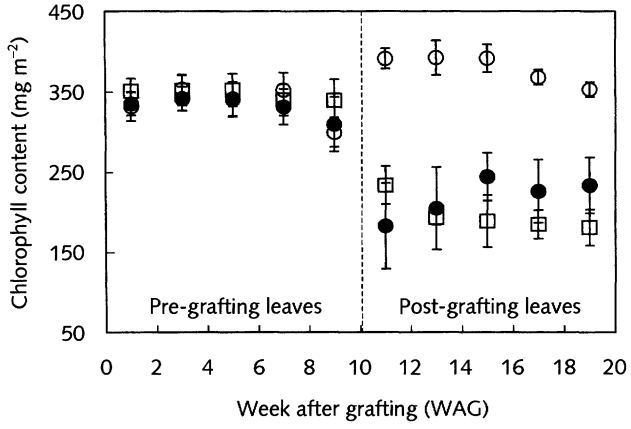

Fig. 1 Chl content of fully expanded *Catharanthus roseus* leaves determined from a calibration curve of SPAD-Chl content measurements, for control (open circle), AshY2 (closed circle), AshY5 (open square). From 1 to 9 wk after grafting (WAG), measurements were obtained from leaves 2 nodes directly below the graft union. From 11 WAG onwards, measurements were obtained from leaves formed after inoculation. Each data point is a mean of 3 replicates. Vertical bars denote ± SE of mean.

of the axillary shoots and with small virescent flowers had formed in several of the AshY5 phytoplasma-infected plants, but these symptoms did not appear in AshY2-infected plants, even up to 19 WAG.

Leaf Chl and N contents

The Chl content of leaves directly below the graft union did not differ between control and diseased treatments for the first 9 WAG (Fig. 1), at which time the mature leaves of inoculated and control plants began to senesce. Senescence was operationally defined as the point when leaves turned soft, chlorotic and drooped from the stem. From wk 11 onwards, leaves that had formed during disease development were monitored. These leaves were about 2–3 wk younger than the leaves used from 1 to 9 WAG. Between 11 and 19 WAG, the Chl content of leaves in the diseased plants was 50–55% that of the control leaves, significantly lower ($P = 0.05$) than that of the control plants. By contrast to the AshY5 treatment, Chl content of the AshY2 treatment showed a slight upward trend between 11 and 19 WAG, such that Chl content was higher than the AshY5 treatment from 13 WAG onwards, even though the differences were not significantly different.

We further determined the Chl contents of leaves three nodes above and below the leaf monitored (at node 5) (Fig. 2) to quantitatively characterize the development of chlorosis on a shoot. Leaves at nodes 2 and 3 were young rapidly expanding leaves between 11 and 13 WAG, whereas those at the remaining nodes were maturing or mature source leaves at 11 WAG. The Chl contents of leaves at all sampled nodes on the control plants remained constant over the 8-wk period (Fig. 2a). By contrast, the Chl content of leaves decreased from older leaves to younger leaves in the AshY5 treatment (Fig. 2c). In addition,

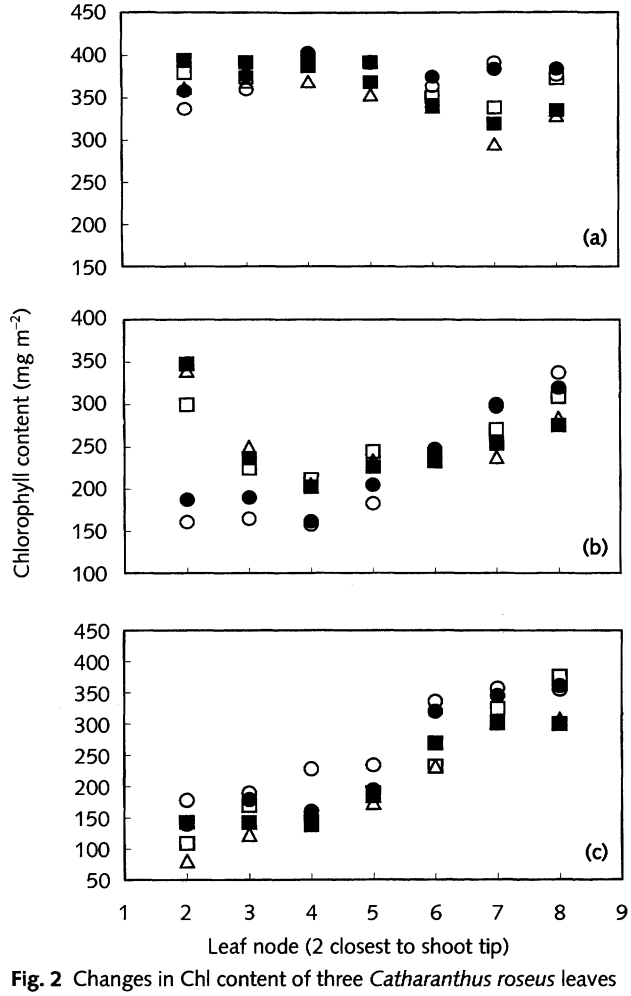

Fig. 2 Changes in Chl content of three *Catharanthus roseus* leaves above and below the leaf used for gas exchange and chlorophyll fluorescence measurements (at node 5), for (a) control (b) AshY2 (c) AshY5 treatment. Chl content of leaves within each treatment are for wk 11 (open circle), wk 13 (closed circle), wk 15 (open square), wk 17 (closed square), and wk 19 (open triangle) after grafting. Chlorophyll contents were determined indirectly from chlorophyll meter. Each data point is a mean of 3 replicates.

the Chl contents of the young expanding leaves decreased with time, compared with the increase in Chl content of the corresponding leaves in the control treatment. In the AshY2 treatment, Chl content increased after 13 WAG for leaves at nodes 2 and 3 (Fig. 2b). Total leaf N as a percentage of the d. wt was determined at 5-wk intervals. The N levels ranged between 3 and 5% of leaf d. wt, and there were no differences between the 3 treatments (data not shown).

Gas exchange

Gas exchange variables of mature leaves two nodes below the graft union showed no differences between treatments over the 8-wk period. For leaves formed after grafting in the AshY5 treatment, net photosynthesis rates at ambient [CO_2] (A_a) of

Table 1 Effects of phytoplasma infection on light saturated net photosynthesis rate at ambient [CO_2] (A_a), and saturated [CO_2] (A_{max}) of *Catharanthus roseus* leaves formed after grafting. A_a and A_{max} of AshY2 and AshY5 treatments are expressed as percentages of the corresponding mean A_a and A_{max} of the control. Values for 1–9 wk after grafting (WAG) were not significantly different between treatments and are not shown

	A_a (% of control)		A_{max} (% of control)	
WAG	AshY2	AshY5	AshY2	AshY5
11	45.5 ± 4.76*	40.5 ± 5.77*	57.0 ± 11.1*	46.1 ± 3.53*
13	71.5 ± 0.64*	42.9 ± 4.97*	81.3 ± 3.99	48.2 ± 7.99*
15	78.9 ± 4.64*	47.6 ± 4.49*	89.9 ± 6.89	58.0 ± 1.47*
17	68.9 ± 8.06*	50.8 ± 11.1*	91.8 ± 11.1	62.4 ± 9.19*
19	80.7 ± 17.4	50.8 ± 7.74*	87.8 ± 12.8	54.0 ± 8.97*

Values shown are means of 3 replicates ± SE of the mean. Asterisk (*) indicates significance between the AshY2 or AshY5 treatment and control at $P = 0.05$.

leaves were 41–51% of the control ($P = 0.05$) (Table 1). A_a was higher in the AshY2 than in the AshY5 treatment, and increased from 45 to 81% of the control between 11 and 19 WAG. Net photosynthesis rate at saturated [CO_2] (A_{max}) of the AshY5 treatment showed the same trend as A_a. On the other hand, the normalized A_{max} of AshY2 treatment were not significantly different from that of the control from 13 WAG onwards, and were higher than the normalized A_a values at each corresponding week.

There was no significant difference in stomatal conductance (G_s) between the treatments from 1 to 9 WAG (Fig. 3a). G_s of the three treatments declined gradually over the 10-wk period, presumably as a result of leaf ontogeny. From 11 WAG onwards, G_s was significantly higher in control plants than the diseased treatments at $P = 0.05$. G_s of the AshY5 treatment was 20% of control leaves on 11 WAG, but was 46% of control leaves by 19 WAG due to the more rapid decrease in G_s of the control treatment. G_s of the AshY2 treatment was higher than the AshY5 treatment, but the difference was not significant at $P = 0.05$, except on 13 WAG, and increased dramatically between 11 and 13 WAG. On 19 WAG, the response of the stomata to leaf-to-air vapor pressure deficit (vpd) for the three treatments was studied by varying the vpd in the leaf chamber from 0.7 to 2.6 kPa (Fig. 3b). The control treatment had higher G_s, followed by the AshY2 treatment across the range of vpd applied to the leaf chamber. Linear regression analysis indicated statistical significance of the regression functions fitted to the data for control ($P < 0.05$), AshY2 ($P < 0.05$) and AshY5 ($P < 0.07$). However, the slopes of the curve were not significantly different between treatments ($P > 0.49$), indicating a similar sensitivity of the stomata to vpd.

The increased diffusional resistances to CO_2 in the diseased treatments did not increase the limitation to photosynthesis. While G_s was significantly lower in diseased plants, there were

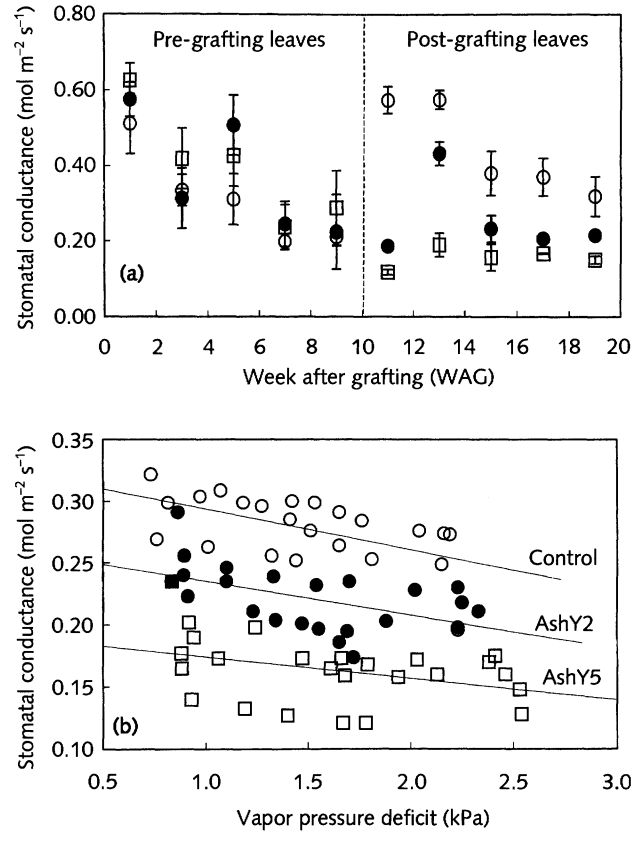

Fig. 3 (a) Stomatal conductance of *Catharanthus roseus* leaves of control (open circle), AshY2 (closed circle), AshY5 (open square) measured under ambient [CO_2] and saturating light level. From 1 to 9 wk after grafting (WAG), measurements were obtained from leaves at 2 nodes directly below the graft union. From 11 WAG onwards, measurements were obtained from leaves formed after inoculation. Each data point is a mean of 3 replicates. Vertical bars denote ± SE of mean. (b) Responses of stomatal conductance to increasing leaf-to-air vapor pressure deficit of the leaf chamber of the gas exchange system, at ambient [CO_2] and saturating light level, for plants at 19 WAG. Labelled lines indicate the linear functions fitted to data points for each treatment. Each data point is a single measurement.

no consistent trends in L_s among treatments over time (Table 2). This result correlated with a lack of difference in C_i at ambient [CO_2] between the treatments (Table 2), except on 13 WAG between AshY2 and control. C_i in the diseased treatments, particularly AshY5, was either the same or higher than in the control plants.

Vc_{max} and J_{max} were used to estimate the biochemical limitations on photosynthesis imposed by the rate of carboxylation and the rate of regeneration of RuBP, respectively. Fig. 4 shows typical A/C_i curves that were obtained. The changes in Vc_{max} and J_{max} derived from the curves at each measurement week are shown in Fig. 5. As with the other parameters measured, there were no treatment differences in Vc_{max} and J_{max} for leaves directly below the graft union. For leaves formed postgrafting, Vc_{max} of the AshY5 treatment was 40–47% of the control treatment, and J_{max} was 38–45%

Table 2 Stomatal limitation index (L_s) and intercellular [CO_2] (C_i) at ambient [CO_2] obtained from gas exchange measurements and A/C_i analysis. Values for 1–9 wk after grafting (WAG) were not significantly different between treatments and are not shown

	L_s	C_i
11 WAG		
Control	27.9 ± 2.48	234 ± 2.08
AshY2	36.7 ± 3.92	233 ± 7.72
AshY5	33.4 ± 2.56	241 ± 2.33
13 WAG		
Control	30.5 ± 2.67	235 ± 2.35
AshY2	24.2 ± 2.30	262 ± 7.78 *
AshY5	28.2 ± 0.83	249 ± 3.33
15 WAG		
Control	31.3 ± 2.36	221 ± 10.1
AshY2	36.9 ± 4.80	240 ± 1.26
AshY5	31.0 ± 0.59	234 ± 9.45
17 WAG		
Control	28.2 ± 2.55	242 ± 7.65
AshY2	32.9 ± 3.14	234 ± 9.45
AshY5	21.3 ± 2.35	273 ± 8.09
19 WAG		
Control	30.8 ± 1.34	233 ± 5.48
AshY2	29.3 ± 2.16	243 ± 4.21
AshY5	23.9 ± 3.64	263 ± 12.4

Values shown are means of 3 replicates ± SE of the mean. The parameters were not significantly between AshY2 or AshY5 and control at $P = 0.05$, except for figure marked with asterisk (*).

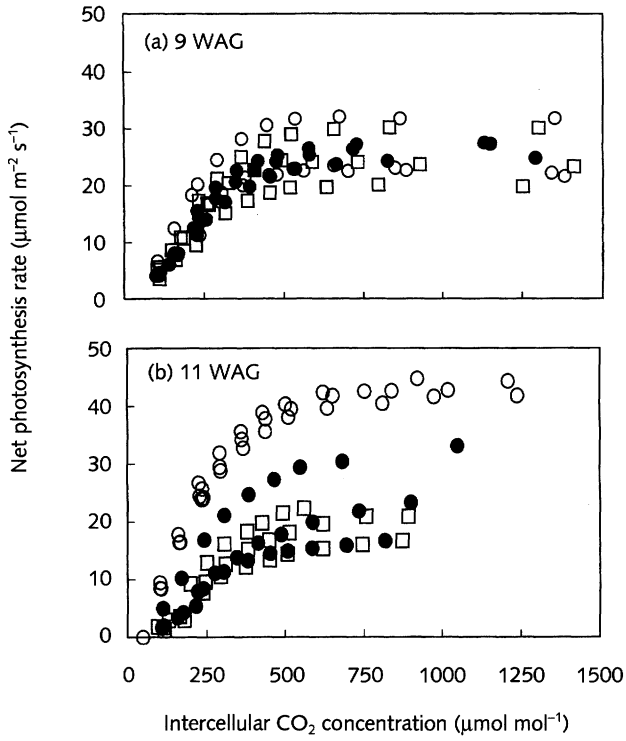

Fig. 4 Net photosynthesis rate (A) vs intercellular CO_2 concentration (C_i) (A/C_i curves) of *Catharanthus roseus* leaves on (a) wk 9 and (b) wk 11 after grafting, obtained by varying the external [CO_2] at saturating light level. From 1 to 9 WAG, measurements were obtained from leaves 2 nodes directly below the graft union. From 11 wk after grafting (WAG) onwards, measurements were obtained from leaves formed after inoculation. Symxbols represent control (open circle), AshY2 (closed circle), AshY5 (open square). Each data point represents a single measurement.

that of the control treatment. The differences were significant at $P = 0.05$. For AshY2 treatment, Vc_{max} was significantly lower than the control at $P = 0.05$, whereas J_{max} was similar to that of the control from 15 WAG.

To determine if ABA was involved in the decrease of G_s in the diseased treatments, leaf ABA concentrations were assayed. There was no significant difference in ABA concentrations among treatments over the experimental period (data not shown). A comparison was also made between the ABA concentrations in the diseased treatments and ABA concentrations in detached healthy leaves allowed to wilt in the greenhouse for 2 h. The ABA concentration in the wilted leaves were 2–2.5 times that of the diseased and healthy control leaves, further indicating that ABA concentrations were not correlated with the decline in G_s of diseased leaves.

Chl fluorescence

Chl fluorescence parameters were monitored to determine the energy state of PSII in conjunction with the biochemical limitations revealed by A/C_i analysis. F_v/F_m of the AshY5 treatment, a measure of the maximum photochemical efficiency of PSII and the degree of photoinhibition, was about 92% that of the control treatment between 11 and 17 WAG. The difference was significant at $P = 0.05$ (Table 3). F_v/F_m of AshY2 treatment were not significantly different from that of the control treatment between 13 and 17 WAG. From 11 to 13 WAG, the lower F_v/F_m of the AshY5 treatment was a result of higher F_o and lower F_m, whereas from 15 to 17 WAG, the lower F_v/F_m was mostly attributed to the lower F_m. Quantum yield of PSII (Φ_{PSII}) at 1980 μmol m^{-2} s^{-1} of PPFD showed the same differences among treatments as F_v/F_m. The lower Φ_{PSII} in the AshY5 treatment was attributed to both lower F_s and lower F'_m, and as with the decline in F_v/F_m, the change in F'_m was greater than F_s with respect to the control (data not shown). Nonphotochemical energy dissipation (q_{NP}) was consistently higher in the AshY5 treatment at $P = 0.05$ than in the control and AshY2.

Discussion

Chl synthesis and degradation

Chlorosis was the first visual symptom of disease development in AshY-infected periwinkles, and is a consistent symptom in

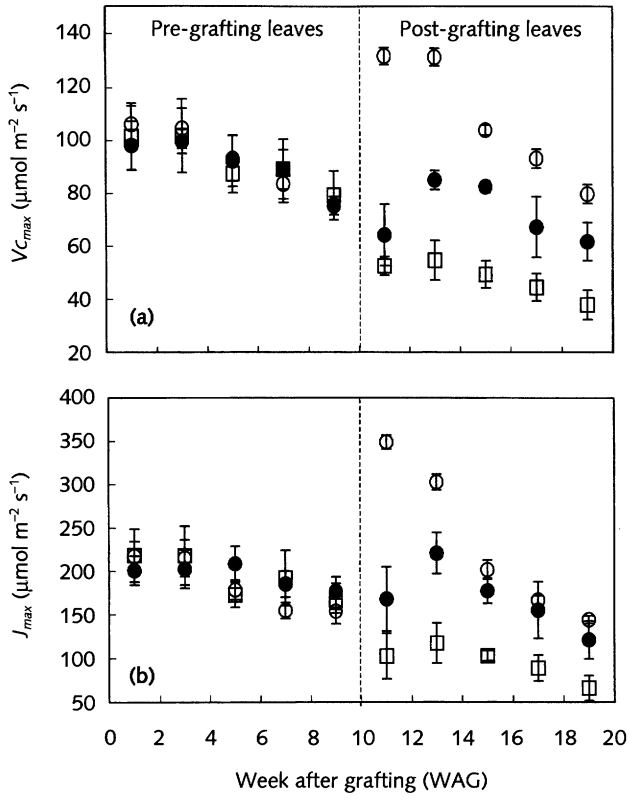

Fig. 5 (a) Maximum rate of carboxylation (Vc_{max}), and (b) maximum rate of electron transport (J_{max}) of *Catharanthus roseus* leaves estimated by fitting the biochemical model of photosynthesis (von Caemmerer & Farquhar, 1981) to A/C_i curves obtained by varying external [CO_2] at saturating light level. From 1 to 9 wk after grafting (WAG), measurements were obtained from leaves 2 nodes below the graft union. From 11 WAG onwards, measurements were obtained leaves formed after inoculation. Symbols represent control (open circle), AshY2 (closed circle), AshY5 (open square). Each data point is a mean of 3 replicates. Vertical bars denote ± SE of the mean.

periwinkle infected by other phytoplasmal strains (Lepka *et al.*, 1999; Sinclair & Griffiths, 2000). Chlorosis is associated with a net loss of Chl, which is a function of the rates of Chl synthesis and Chl degradation. Since Chl synthesis is a major process in young expanding leaves, and decreases with leaf age (Hendry *et al.*, 1987), reduced Chl synthesis will be most pronounced in young expanding leaves. Infection by AshY5 phytoplasma apparently inhibited Chl synthesis in the young expanding leaves. Chl content of the young expanding leaves (at nodes 2 and 3) (Fig. 2c) declined gradually as leaf expansion proceeded, which differed with the gradual increase in Chl contents of leaves at the corresponding nodes in the control treatment (Fig. 2a). The AshY2-inoculated plants appeared to recover partially from the infection from 13 WAG. In the treatment, the Chl content of leaves at nodes 2 and 3 increased dramatically (Fig. 2b), presumably as a result of a resumption of Chl synthesis. In leaves formed after grafting, there appeared to be a similar rate of Chl degradation in diseased and healthy plants (Fig. 1). Therefore, in these leaves, the lower Chl content in the diseased treatment at 11 WAG might then be due to inhibition of Chl synthesis as the leaves were expanding.

In periwinkle infected with dwarf aster yellows and severe aster yellows, chlorosis was also most severe in young expanding leaves (Kuske & Kirkpatrick, 1992). However, Lepka *et al.* (1999) obtained a different result, in which AshY1-infected periwinkle developed most severe chlorosis in the fifth leaf, which was a mature source leaf, whereas the young leaves were still green. Possibly, this difference resulted from unknown phytoplasma strain-specific factors. Kuske & Kirkpatrick (1992) reported similar differences in periwinkle infected with the severe and dwarf strains of aster yellows phytoplasmas. In our study, the more severe chlorosis in young leaves, as well as the development of symptoms in leaves formed during disease development but not mature leaves present at the time of grafting, is consistent with the hypothesis that at least in some phytoplasmal infections, pathogenesis occurs through a localized effect in sink tissues in which phytoplasma had accumulated or multiplied preferentially. Leisner *et al.* (1992) demonstrated a close correlation between photoassimilate accumulation and preferential translocation of cauliflower mosaic virus into young leaves. We postulated a similar relationship between phloem transport of photoassimilate and movement of phytoplasma into young sink leaves, with the corollary that phytoplasma would be present in mature leaves in relatively lower quantities. While direct quantification of phytoplasma would be needed to demonstrate a conclusive link between symptom severity and localized phytoplasmal titre, our results support this hypothesis as opposed to the alternative, whereby symptom expression is remote from the site of action. This indicates that the mode of pathogenicity of AshY is similar to severe and dwarf strains of western aster yellows (Kuske & Kirkpatrick, 1992) and eastern X disease phytoplasmas (Douglas, 1986) diseases, whereby overt symptoms were suggested to occur via metabolic perturbations arizing from a localized accumulation of phytoplasmas. In other phytoplasmal diseases in which mature leaves also develop symptoms, pathogenesis was suggested to occur via a translocated phytoplasma-derived or phytoplasma-induced metabolite (Nakashima & Hayashi, 1995; Siddique *et al.*, 1998).

Absence of increased stomatal limitation on photosynthesis

Reduced stomatal conductance is an early symptom in disease development (Matteoni & Sinclair, 1983). However, our results did not support the hypothesis that reduced stomatal conductance increased the stomatal limitation on photosynthesis early in disease development. To conclude that reduced stomatal conductance is dominant in the response of A to some perturbation, C_i should change in the same

Table 3 Chl fluorescence parameters: dark adapted minimal fluorescence (F_o), dark adapted maximum fluorescence (F_m), maximum quantum efficiency of PSII (F_v/F_m), quantum efficiency of PSII at 1980 μmol m^{-2} s^{-1} PPFD (Φ_{PSII}), nonphotochemical quenching (q_{NP}) for *Catharanthus roseus* leaves formed after grafting

Fluorescence parameters	F_o	F_m	F_v/F_m	Φ_{PSII}	q_{NP}
11 WAG					
Control	89.7 ± 1.92	603 ± 12.8	0.85 ± 0.00	0.61 ± 0.02	0.54 ± 0.04
AshY2	138 ± 11.7*	544 ± 97.8	0.71 ± 0.08*	0.41 ± 0.07*	0.82 ± 0.08*
AshY5	135 ± 2.17*	544 ± 56.8	0.75 ± 0.03*	0.35 ± 0.05*	0.80 ± 0.13*
13 WAG					
Control	82.7 ± 1.17	616 ± 15.7	0.87 ± 0.00	0.65 ± 0.01	0.54 ± 0.02
AshY2	77.0 ± 6.24	581 ± 50.7	0.87 ± 0.00	0.54 ± 0.02	0.57 ± 0.11
AshY5	111 ± 13.0	577 ± 7.04	0.81 ± 0.02*	0.37 ± 0.07*	0.84 ± 0.05*
15 WAG					
Control	93.0 ± 0.58	676 ± 23.1	0.86 ± 0.01	0.52 ± 0.01	0.70 ± 0.02
AshY2	88.0 ± 5.20	623 ± 33.5	0.86 ± 0.00	0.52 ± 0.02	0.78 ± 0.04
AshY5	94.7 ± 4.37	529 ± 117	0.81 ± 0.03*	0.37 ± 0.03*	0.86 ± 0.04*
17 WAG					
Control	89.0 ± 3.51	638 ± 41.6	0.86 ± 0.01	0.46 ± 0.05	0.73 ± 0.02
AshY2	86.2 ± 12.4	548 ± 72.3	0.84 ± 0.02	0.45 ± 0.09	0.66 ± 0.06
AshY5	98.3 ± 12.9	456 ± 49.9	0.79 ± 0.01*	0.33 ± 0.05	0.86 ± 0.01*

Values for 1–9 WAG were not significantly different between treatments and are not shown. Values shown are mean of 3 replicates ± SE of the mean. Asterisk (*) indicates significance between AshY2 or AshY5 treatment and control at $P = 0.05$.

direction as A and L_s should increase relative to the control (Farquhar & Sharkey, 1982). However, C_i in the diseased plants was either similar to or higher than in healthy plants (Table 2). A higher C_i reflects the lack of demand for CO_2 by the photosynthetic carbon reduction cycle resulting from biochemical limitations to photosynthesis.

G_s is a function of stomatal frequency and stomatal pore area. Stomatal pore area in turn depends on the stomatal aperture, which is generally determined by the stomatal pore width and the inherent size of the guard cell (determined by the guard cell width, length and depth) (Weyers & Meidner, 1990). Therefore, reduced G_s could result from reduced stomatal frequency, reduced pore area, or both factors. Reduced stomatal pore width was demonstrated in several phytoplasma diseases, including periwinkle infected with AshY phytoplasma using leaf surface replicas (Matteoni & Sinclair, 1983). It is unknown whether stomatal frequency and stomatal pore area (as a function of guard cell size) were affected in leaves formed after infection. However, since profound hormonal imbalance is implicated in the formation of witches' brooms, reduced leaf sizes and shorter internodes (Davis & Lee, 1982; Kuske & Kirkpatrick, 1992), leaf developmental processes including stomata initiation and differentiation could be similarly affected. Stomatal frequency and guard cell size are known to be affected by developmental stage of the leaves, and external factors such as nutrition and water status (Tichá, 1982). Even when a low vpd was imposed to stimulate stomatal opening, the G_s in diseased plants was lower than the healthy plants, and the difference in the average G_s was maintained across the entire range of vpd imposed (Fig. 3b). This suggests that leaves formed during pathogenesis had developed a lower total stomatal pore area per unit leaf area independent of stomatal closure or opening, thereby contributing to an inherently lower G_s compared with the control plants. However, we did not find convincing evidence of altered stomatal frequency or guard cell size in diseased leaves of periwinkle, *Fraxinus pennsylvanica* and *Ulmus* in a preliminary study (data not shown). Nevertheless, the effects of infection on stomatal frequency, stomatal pore area and other leaf developmental processes deserve further study.

The lower G_s in the diseased treatments was also not due to an increased leaf ABA concentration. León *et al.* (1996) and Martinez *et al.* (2000) arrived at the same conclusion in their study of lethal yellowing of coconut palms. Although ABA concentration increased in lethal yellowing-diseased coconut palms, the increase occurred only when G_s in diseased palms had dropped to *c.* 20% that of symptomless palms. In our study, any increase in ABA concentration in the transpiration stream will likely lead to lower G_s in the mature leaves, which was not observed, further indicating that ABA concentration was not altered. While ABA has been extensively studied as the main messenger to environmental stresses that promote stomatal closure, Lu *et al.* (1997) recently proposed an alternative mechanism whereby sucrose accumulation in the apoplast of guard cells leads to stomatal closure. Following sucrose accumulation, the eventual uptake of sucrose into the guard cells via the sucrose-proton symport is expected to lead to membrane depolarization of the guard cell plasma membrane.

This is similar to ABA-induced membrane depolarization, which leads to an efflux of K^+ and a cascade of processes leading to stomatal closure (Leung & Giraudat, 1998). Two factors increase sucrose accumulation in the guard cell apoplast: increased transpiration and reduced translocation of sucrose from the surrounding mesophyll cells (Lu *et al.*, 1997). The first factor is unlikely to occur in symptomatic leaves because reduced G_s is the rule, and diseased plants often have more positive leaf water potential (Matteoni & Sinclair, 1983). However, there is a correlation between increased accumulation of soluble sugars (including sucrose) and reduced G_s in symptomatic leaves of periwinkle infected with AshY5 phytoplasma (unpublished data). Lepka *et al.* (1999) similarly reported the accumulation of sucrose in periwinkle infected with several strains of phytoplasma. If the sucrose retention in the mesophyll cells leads to an accumulation of sucrose in the guard cell apoplast, the observed reduced G_s may occur via the mechanism suggested by Lu *et al.* (1997).

Patchy stomatal closure has been shown to lead to erroneous calculations of C_i by gas exchange methods (Terashima *et al.*, 1988). We cannot be certain that stomatal patchiness did not develop with disease development during the gas exchange measurements, yet we submit that stomatal patchiness seemed unlikely. This is because disease development took up to 8 wk, whereas stomatal patchiness is most frequently associated with the rapid onset of environmental stresses, especially those associated with water stress and the corresponding increases in ABA concentration (Beyschlag & Eckstein, 1998).

Biochemical limitations to photosynthesis

It was possible to distinguish between the biochemical limitations imposed by Vc_{max} from J_{max} in AshY2 infected plants. There appeared to be a recovery from the infection from 13 WAG onwards, but the recovery was partial as A and Vc_{max} were still lower compared with the control up to 17 WAG. However, the noncyclic electron transport capacity of the thylakoids indicated by J_{max} was similar to the control by 15 WAG (Fig. 5b), and so RuBP regeneration rate by that stage was not limiting photosynthesis. Likewise, F_v/F_m indicated that the intrinsic efficiency of PSII in the utilization of absorbed photons was equivalent to the control by 13 WAG. In the biochemical model used, the regeneration of RuBP was solely dependent on the rate of electron transport required for generation of energy and reducing equivalents ATP and NADPH. However, it should be noted that RuBP regeneration is also dependent on the activities of the photosynthetic carbon reduction cycle enzymes that convert the triose phosphates to RuBP, and sink activity which determines the utilization rate of end products of photosynthesis (Bowes, 1996; Genty & Harbinson, 1996). Therefore, the sum of these factors may have contributed to the resumption of RuBP regeneration capacity in the AshY2 treatment. The carboxylation capa-city of Rubisco is determined by both its activation state in the carbamylated form (von Caemmerer & Farquhar, 1981; Brooks, 1986; Woodrow & Mott, 1989; Sawada *et al.*, 1990) as well as the quantity of the enzyme (von Caemmerer & Farquhar, 1981; Brooks, 1986). Since more than half of leaf N is usually associated with the photosynthetic enzymes and proteins for light harvesting and electron transport (Evans & Seemann, 1996), there is usually a close correlation between leaf N content and photosynthetic properties (Evans, 1989; Kull & Niinemets, 1998). We found no difference in leaf N expressed as a percentage of d. wt between the treatments. This could indicate that the lower Vc_{max} reflected a lower activation state of Rubisco, and not a lower Rubisco content. Alternatively, if the phytoplasma sequestered N available to host cells, the total N detected would be the same between the treatments, but with a consequent reduction in N availability to the host. Clearly, the interaction between phytoplasma, leaf N and photosynthesis can be potentially complex. Such a three–way interaction was also suggested to complicate the study of plant viral infections (Balachandran *et al.*, 1997). Nevertheless, it seemed clear that the reduced net photosynthesis rate of the AshY2 treatment was a consequence of reduced carboxylation by Rubisco. The fact that A_{max} was consistently higher than the corresponding A_a (Table 1) provides further evidence that during recovery, the limitation of photosynthesis by the rate of end-product synthesis via a feedback inhibition mechanism was not as important as the limitation by the initial carboxylation step of the Calvin cycle (Krapp *et al.*, 1991).

In plants affected by the more aggressive AshY5 phytoplasma, reduced photosynthesis was due to sustained reductions in both the carboxylation capacity as well as the regeneration of RuBP, which suggest a down-regulation of the Calvin cycle activities. However, it was not evident from the data which factor was affected first following infection, as Vc_{max} and J_{max} expressed as percentages of the control were similar in range at each WAG, and there was no apparent difference in the rate of decline of the variables over time (Fig. 5). With reduced carboxylation capacity, it is expected that there will be an imbalance between photon absorption and photon utilization through photochemistry. The sustained depression in F_v/F_m between 11 and 17 WAG indicated that photoinhibition had occurred. Photoinhibition results from either oxidative damage to D1 protein and other components of the PSII reaction centres resulting from generation of reactive O_2 species, or a photoprotective process involving alteration of the PSII reaction centres which convert more of trapped energy to heat (Krause, 1988). Sustained decreases in F_v/F_m and F_m, accompanied by a substantial increase in F_o indicate irreversible inactivation of the PSII reaction centres, with part of the centres losing their function as energy traps. PSII inactivation is considered reversible if PSII is inactivated via conversion of the reaction centres to fluorescence quenchers that convert the excitation energy to heat, and will be reflected in decreases in F_v/F_m, F_m and F_o. The increase in thermal

dissipation of the excitation energy is then a photoprotective mechanism and is the most important component of q_{NP} (Horton *et al.*, 1996). The increased thermal dissipation of the excitation energy was reflected in the significantly higher q_{NP} in AshY5 infected leaves, compared with the control. Even though F_o was initially higher in the AshY5 and AshY2 treatments on 11 WAG, F_o decreased subsequently to levels not significantly different from the control, and the decrease in F_m compared with control treatment was substantially higher. This indicates that the observed photoinhibition was likely due to photoprotective processes rather than photooxidative damage to the PSII reaction centres. In the AshY2 treatment, the rapid decrease in F_o after 11 WAG also indicates efficient repair to the possible damaged reaction centres coinciding with the recovery phase. Under prolonged exposure to excess photon absorption, photobleaching of chlorophyll also results from severe inactivation or dsestruction of the reaction centres (Krause, 1988). That photobleaching of Chl in the diseased leaves (in comparison with healthy leaves) was not observed further indicated the lack of photooxidative damage.

Since light harvesting and photochemistry of photosynthesis are coupled (Owens, 1996), the sustained decrease in F_v/F_m may also reflect the down regulation of photochemistry. This occurs due to the reduced demand for NADPH and ATP resulting from reduced activities of the Calvin cycle, which in turn leads to a reduction in the electron carriers of PSII and PSI (Owens, 1996). This process has also been suggested to account for the decline in F_v/F_m in peach leaves infected with the fungus *Taphrina deformans* (Raggi, 1995). The reduced Calvin cycle activities may in turn result from carbohydrate accumulation that was observed in diseased leaves (unpublished data), in that the accumulation of carbohydrate leads to a general down-regulation of photosynthesis by repression of genes of the photosynthetic machinery (Krapp *et al.*, 1991). This has been suggested in viral infection (Balachandran *et al.*, 1997) and several fungal infections (Scholes *et al.*, 1994; Tang *et al.*, 1996). Whether or not such a phenomenon occurs in phytoplasmal diseased remains to be studied.

There was a clear distinction in the severity of disruption of the normal physiological processes after infection by AshY phytoplasmas of different aggressiveness. This result may stem from the different degrees of host responses to particular strains of phytoplasma, or different pathogenicity factors specific to the phytoplasma strains. The underlying causes of differences in aggressiveness of phytoplasma strains are not yet known (Sinclair & Griffiths, 2000). However, the difference in aggressiveness of AshY2 and AshY5 phytoplasmas may relate to the level of accumulation of the phytoplasma in affected leaves, which in turn depends on the rate of multiplication of the phytoplasma and the rate of movement from the infection source. Such a conclusion is supported by the notion that the severity of symptom expression correlates with the level of phytoplasma accumulation. Alternatively, host factors may suppress symptom development in plants affected by a less aggressive strain such as AshY2, and it has been observed that healthy plants grafted with scions containing weaker strains of phytoplasma do occasionally remain nonsymptomatic (W. A. Sinclair, personal communication). Siddique *et al.* (1998) suggested that tissue necrosis observed in dieback-affected papaya was a result of a hypersensitive response triggered by the presence of phytoplasma, leading to a containment and eventual destruction of phytoplasma in the necrotic tissue. Musetti *et al.* (1999) also suggested that an observed increase in polyamines in phytoplasma-infected periwinkle tissue, which are implicated in the hypersensitive response towards viral and fungal infection, could play a role in the plant defense responses leading to recovery from the disease.

In conclusion, known differences in AshY phytoplasmal aggressiveness based on growth studies correlated with the severity of the effects of the phytoplasmal infection on chlorophyll synthesis, carboxylation capacity of Rubisco, electron transport capacity of the thylakoids and chlorophyll fluorescence characteristics of symptomatic leaves. AshY phytoplasmas appear to cause metabolic perturbations via localized accumulation or multiplication in symptomatic leaves. Although stomatal closure is an early symptom of phytoplasmal disease development, stomatal limitation of photosynthesis imposed by stomatal closure did not increase with respect to healthy plants. We suggest that the reduced stomatal conductance was a consequence rather than a cause of reduced photosynthesis. The reduced stomatal conductance was not associated with changes in ABA concentration, and could arise from both stomatal closure due to sucrose accumulation, as well as reductions in stomatal frequency and guard cell size during leaf ontogeny in a systemically infected plant. Reduced photosynthesis was a result of reduced carboxylation capacity of Rubisco and reduced regeneration rate of RuBP, indicating a down-regulation of the Calvin cycle. The reduction in F_v/F_m was likely to be due to increased activities of photoprotective processes and not photooxidative damage to the PSII thylakoids.

Acknowledgements

We thank W. A. Sinclair and H. M. Griffiths for the phytoplasma strains, periwinkle and their helpful comments on the experiment, T. L. Setter for assistance with the ABA and carbohydrate assays, T. G. Owens for the use of the FMS2, R. Wayne for the use of the image analysis system, and C. Olsen for assistance with nonlinear regression analysis of the A/C_i data. We thank all the above and R. E. Turgeon for their constructive comments on the manuscript.

References

Balachandran S, Osmond CB. 1994. Susceptibility of tobacco leaves to photoinhibition following infection with two strains of tobacco mosaic

virus under different light and nitrogen nutrition regimes. *Plant Physiology* **104**: 1051–1057.

Balachandran S, Hurry VM, Kelley SE, Osmond CB, Robinson SA, Rohozinski J, Seaton GGR, Sims DA. 1997. Concepts of plant biotic stress. Some insights into the stress physiology of virus-infected plants, from the perspective of photosynthesis. *Physiologia Plantarum* **100**: 203–213.

Beyschlag W, Eckstein J. 1998. Stomatal patchiness. *Progress in Botany* **59**: 283–298.

Bowes G. 1996. Photosynthetic responses to changing atmospheric carbon dioxide concentration. In: Baker NR, ed. *Photosynthesis and the environment.* Dordrecht, The Netherlands: Kluwer Academic Press, 387–407.

Brooks A. 1986. Effects of phosphorus nutrition on ribulose-1,5-bisphosphate carboxylase activation, photosynthetic quantum yield and amounts of some Calvin-cycle metabolites in spinach leaves. *Australian Journal of Plant Physiology* **13**: 165–177.

Davis RE, Lee IM. 1982. Pathogenicity of spiroplasmas, mycoplasmalike organisms, and vascular-limited fastidious walled bacteria. In: Mount MS, Lacy GH, eds. *Phytopathogenic prokaryotes.* New York, USA: Academic Press, 492–509.

Douglas SM. 1986. Detection of mycoplasmalike organisms in peach and chokeberry with X-disease by fluorescence microscopy. *Phytopathology* **76**: 784–787.

Evans JR. 1989. Photosynthesis and nitrogen relationships in leaves of C_3 plants. *Oecologia* **78**: 9–19.

Evans JR, Seemann JR. 1996. The allocation of protein nitrogen in the photosynthetic apparatus: costs, consequences, and control. In: Baker NR, ed. *Photosynthesis and the environment.* Dordrecht, The Netherlands: Kluwer Academic Press, 183–205.

Farquhar GD, Sharkey TD. 1982. Stomatal conductance and photosynthesis. *Annual Review of Plant Physiology* **33**: 317–345.

Geber MA, Dawson TE. 1997. Genetic variation in stomatal and biochemical limitations to photosynthesis in the annual plant, *Polygonum arenastrum. Oecologia* **109**: 535–546.

Genty B, Braintais JM, Baker NR. 1989. The relationship between the quantum yield of photosynthetic electron transport and quenching of Chl fluorescence. *Biochimica et Biophysica Acta* **990**: 87–92.

Genty B, Harbinson J. 1996. Regulation of light utilization for photosynthetic electron transport in vivo. In: Baker NR, ed. *Photosynthesis and the environment.* Dordrecht, The Netherlands: Kluwer Academic Press, 68–92.

Gilbertson RL, Lucas WJ. 1996. How do viruses traffic on the 'vascular highway'? *Trends in Plant Science* **1**: 260–268.

Griffiths HM, Sinclair WA, Smart CD, Davis RE. 1999. The phytoplasma associated with ash yellows and lilac witches'-broom: '*Candidatus* Phytoplasma fraxini'. *International Journal of Systematic Bacteriology* **49**: 1605–1614.

Harley PC, Thomas RB, Reynolds JF, Strain BR. 1992. Modeling photosynthesis of cotton grown in elevated CO_2. *Plant, Cell & Environment* **15**: 271–282.

Hendry GA, Houghton JD, Brown SB. 1987. The degradation of chlorophyll – a biological enigma. *New Phytologist* **107**: 255–302.

Horton P, Ruban AV, Walters RG. 1996. Regulation of light harvesting of green plants. *Annual Review of Plant Physiology and Plant Molecular Biology* **47**: 655–684.

Krapp A, Quick WP, Stitt M. 1991. Ribulose-1,5-bisphosphate carboxylase-oxygenase, other Calvin-cycle enzymes, and chlorophyll decrease when glucose is supplied to mature spinach leaves via the transpiration stream. *Planta* **186**: 58–69.

Krause GH. 1988. Photoinhibition of photosynthesis. An evaluation of damaging and protective mechanisms. *Physiologia Plantarum* **74**: 566–574.

Krause GH, Weis E. 1991. Chlorophyll fluorescence and photosynthesis: the basics. *Annual Review of Plant Physiology and Plant Molecular Biology* **42**: 313–349.

Kull O, Niinemets Ü. 1998. Distribution of leaf photosynthetic properties in tree canopies: comparison of species with different shade tolerance. *Functional Ecology* **12**: 472–479.

Kuske CR, Kirkpatrick BC. 1992. Distribution and multiplication of western aster yellows mycoplasmalike organisms in *Catharanthus roseus* as determined by DNA hybridization analysis. *Phytopathology* **82**: 457–462.

León R, Santamaría JM, Alpizar L, Escamilla JA, Oropeza C. 1996. Physiological and biochemical changes in shoots of coconut palms affected by lethal yellowing. *New Phytologist* **134**: 227–234.

Lepka P, Stitt M, Moll E, Seemüller E. 1999. Effect of phytoplasma infection on concentration and translocation of carbohydrates and amino acids in periwinkle and tobacco. *Physiological and Molecular Plant Pathology* **55**: 59–68.

Leisner SM, Turgeon R, Howell SH. 1992. Long distance movement of cauliflower mosaic virus in infected turnip plants. *Molecular Plant Microbe Interactions* **1**: 41–47.

Leisner SM, Turgeon R. 1993. Movement of virus and photoassimilate in the phloem: a comparative analysis. *Bioassays* **15**: 741–748.

Leung J, Giraudat J. 1998. Abscisic acid signal transduction. *Annual Review of Plant Physiology and Plant Molecular Biology* **49**: 199–222.

Lu P, Outlaw WH, Smith BG, Freed GA. 1997. A new mechanism for the regulation of stomatal aperture in intact leaves. *Plant Physiology* **114**: 109–118.

Martinez S, Cordova I, Maust BE, Santamaria JM. 2000. Is abscisic acid responsible for abnormal stomatal closure in coconut palms showing lethal yellowing? *Journal of Plant Physiology* **156**: 319–322.

Matteoni JA, Sinclair WA. 1983. Stomatal closure in plants infected with mycoplasmalike organisms. *Phytopathology* **73**: 398–402.

Moran R. 1982. Formulae for determination of chlorophyllous pigments extracted with *N,N*-dimethylformamide. *Plant Physiology* **69**: 1376–1381.

Moran R, Porath D. 1980. Chlorophyll determination in intact tissues using *N,N*-dimethylformamide. *Plant Physiology* **65**: 478–479.

Musetti R, Scaramagli S, Vighi C, Pressacco L, Torrigiani P, Favali MA. 1999. The involvement of polyamines in phytoplasma-infected periwinkle (*Catharanthus roseus* L.) plants. *Plant Biosystems* **133**: 37–45.

Nakashima K, Hayashi T. 1995. Multiplication and distribution of rice yellow dwarf phytoplasma in infected tissues of rice and green rice leafhopper *Nephotettix cincticeps. Annals of the Phytopathological Society of Japan* **61**: 451–455.

Ober ES, Setter TL, Madison JT, Thompson JF, Shapiro PS. 1991. Influence of water deficit on maize endosperm development. Enzyme activities and RNA transcripts of starch and zein synthesis, abscisic acid, and cell division. *Plant Physiology* **97**: 154–164.

Owens TG. 1996. Processing of excitation energy by antenna pigments. In: Baker NR, ed. *Photosynthesis and the environment.* Dordrecht, The Netherlands: Kluwer Academic Press, 1–21.

Raggi V. 1995. CO_2 assimilation, respiration and Chl fluorescence in peach leaves infected by *Taphrina deformans. Physiologia Plantarum* **93**: 540–544.

Sage RF. 1994. Acclimation of photosynthesis to increasing atmospheric CO_2: the gas exchange perspective. *Photosynthesis Research* **39**: 351–368.

Samaddar KR, Das J, Barat M, Bhar N, Sengupta C. 1996. Histological and biochemical changes in Mycoplasma infected leaves of eggplant. *Journal of Mycopathology* **34**: 149–155.

Sawada S, Usuda U, Hasegawa Y, Tsukui T. 1990. Regulation of ribulose-1,5-bisphosphate carboxylase activity in response to changes in the source: sink balance in single-rooted soybean leaves: the role of inorganic orthophosphate in activation of the enzyme. *Plant Cell Physiology* **31**: 697–704.

Scholes JD, Lee PJ, Horton P, Lewis DH. 1994. Invertase: understanding changes in the photosynthetic and carbohydrate metabolism of barley leaves infected with powdery mildew. *New Phytologist* **126**: 213–222.

Schreiber U, Schliwa W, Bilger U. 1986. Continuous recording of photochemical and nonphotochemical quenching with a new type of modulation fluorimeter. *Photosynthesis Research* **10**: 51–62.

Seemüller E. 1976. Investigations to demonstrate mycoplasmalike organisms in diseased plants by fluorescence microscopy. *Acta Horticulturae* **67**: 109–112.

Sharkey TD. 1989. Evaluating the role of Rubisco regulation in photosynthesis in C_3 plants. *Philosophical Transactions of the Royal Society of London Series B* **323**: 435–448.

Siddique ABM, Guthrie JN, Walsh KB, White DT, Scott PT. 1998. Histopathology and within-plant distribution of the phytoplasma associated with Australian papaya dieback. *Plant Disease* **82**: 1112–1120.

Sinclair WA, Griffiths HM. 1994. Ash yellows and its relationship to dieback and decline of ash. *Annual Review of Phytopathology* **32**: 49–60.

Sinclair WA, Griffiths HM. 1997. Comparisons of tolerance of ash yellows phytoplasmas in *Fraxinus* species and rootstock-scion combinations. *Plant Disease* **81**: 395–398.

Sinclair WA, Griffiths HM. 2000. Variation in aggressiveness of ash yellows phytoplasmas. *Plant Disease* **84**: 282–288.

Sinclair WA, Griffiths HM, Davis RE. 1996. Ash yellows and lilac witches'-broom: phytoplasmal diseases of concern in forestry and horticulture. *Plant Disease* **80**: 468–475.

Sinclair WA, Griffiths HM, Whitlow TH. 1997. Heritable tolerance of ash yellows phytoplasmas in green ash. *Canadian Journal of Forest Research* **27**: 1928–1935.

Tang X, Rolfe SA, Scholes JD. 1996. The effect of *Albugo candida* (white blister rust) on the photosynthetic and carbohydrate metabolism of leaves of *Arabidopsis thaliana*. *Plant, Cell & Environment* **19**: 967–975.

Terashima I, Wong SC, Osmond CB, Farquhar GD. 1988. Characterization of nonuniform photosynthesis induced b abscisic acid in leaves having different mesophyll anatomies. *Plant Cell Physiology* **29**: 385–394.

Tichá I. 1982. Photosynthetic characteristics during ontogenesis of leaves. 7. Stomata density and sizes. *Photosynthetica* **16**: 375–471.

von Caemmerer S, Farquhar GD. 1981. Some relationships between the biochemistry of photosynthesis and the gas exchange of leaves. *Planta* **153**: 376–387.

Weyers JDB, Meidner H. 1990. *Methods in Stomatal Research*. Essex, UK: Longman Scientific & Technical.

Woodrow IE, Mott KA. 1989. Rate limitation of nonsteady-state photosynthesis by ribulose-1,5-bisphosphate carboxylase in spinach. *Australian Journal of Plant Physiology* **16**: 487–500.